DOI: 10.1002/chem.200700351

Conversion of Perhydropolysilazane into a SiO_x Network Triggered by Vacuum Ultraviolet Irradiation: Access to Flexible, Transparent Barrier Coatings

Lutz Prager,*[a] Andreas Dierdorf,[b] Hubert Liebe,[b] Sergej Naumov,[a] Sandra Stojanović,[b] Roswitha Heller,[a] Luise Wennrich,[a] and Michael R. Buchmeiser*[a, c]

Abstract: The photochemical conversion of 200–500 nm layers of perhydropolysilazane $-(SiH_2\text{-}NH)_n-$ (PHPS) in the presence of oxygen into an SiO_x network was studied. Different UV sources in the wavelength range of 160–240 nm, that is, 172 nm Xe_2^* and 222 nm KrCl* excimer, and 185 nm Hg low-pressure (HgLP) lamps were used for these purposes. The role of both ozone and $O(^1D)$ as well as of catalytic amounts of tertiary amines in the degradation process of PHPS and the formation of SiO_x were studied. In this context, the kinetics of the entire reaction were elucidated and allowed both a continuous and discontinuous process to be established for the production of fully transparent, flexible barrier coatings. Barrier improvement factors (BIFs) of 400 were achieved with one single layer on 23 μm poly(ethylene-terephthalate) (PET), which translated into oxygen transmission rates (OTRs) of $0.20\ cm^3 m^{-2} day^{-1} bar^{-1}$. Double layers prepared by this technique allowed the realization of OTRs of $\leq 0.1\ cm^3 m^{-2} day^{-1} bar^{-1}$, corresponding to BIFs of ≥ 800.

Keywords: barrier layers · photolysis · polysilazanes · silanes · surface chemistry

Introduction

Barrier coatings are of enormous significance in many areas of materials science. Numerous approaches exist for their realization.[1–4] Silica films of 50–500 nm thickness deposited onto polymeric substrates are of significant interest for a broad variety of applications. In fact, the successful realization of numerous high-tech applications such as flexible organic light-emitting diodes or solar cells is highly dependent on the existence of suitable barrier materials that protect these materials against oxygen and moisture. Typical properties of such layers are high transparency, low weight, and high cost-effectiveness associated with good and durable barrier properties against oxygen, water vapor, and aroma.[5–7] Hence, applications range from gas barriers in the packaging industry,[5,7,8] anticorrosive, protective coatings for metal surfaces against water vapor, and oxygen barriers for flexible solar cells,[9,10] multilayer arrangements for applications in electronics,[11] flexible organic light-emitting diodes (OLEDs)[12] and vacuum-insulated panels (VIPs).[13] State of the art for producing such layers are physical vapor deposition (PVD),[14] plasma-enhanced chemical vapor deposition (PECVD),[15,16] reactive sputtering,[17] and sol–gel procedures.[18] Because these techniques may not always be applied to sensitive polymers, alternative processes, preferably ones which can be run at ambient temperature and pressure, need to be developed.

The thermal conversion of perhydropolysilazane (PHPS) in the presence of moisture into SiO_x has already been in-

[a] Dr. L. Prager, Dr. S. Naumov, R. Heller, Dr. L. Wennrich, Prof. Dr. M. R. Buchmeiser
Leibniz-Institut für Oberflächenmodifizierung e.V.
Permoserstrasse 15, 04318 Leipzig (Germany)
Fax: (+43) 341-235-2584
E-mail: lutz.prager@iom-leipzig.de
michael.buchmeiser@iom-leipzig.de

[b] Dr. A. Dierdorf, H. Liebe, Dr. S. Stojanović
Clariant GmbH, Am Unisys-Park 1, 65843 Sulzbach a. T. (Germany)

[c] Prof. Dr. M. R. Buchmeiser
Institut für Technische Chemie, Universität Leipzig
Linnéstrasse 3, 04103 Leipzig (Germany)
Fax: (+43) 341-235-2584

Supporting information (IR transmission spectra (2170 and 1050 cm^{-1}, respectively) of pristine and cured PHPS) for this article is available on the WWW under http://www.chemeurj.org/ or from the authors.

WILEY InterScience DISCOVER SOMETHING GREAT

© 2007 Wiley-VCH Verlag GmbH & Co. KGaA, Weinheim

vestigated.[19,20] PHPS is an inorganic oligomer ($M_n = 600$–$2000\,g\,mol^{-1}$, $M_w = 1400$—$10\,000\,g\,mol^{-1}$, polydispersity index (PDI) 2.3–5) consisting of different $-(SiH_2\text{-}NH)-$ units arranged in a cyclic fashion.[19] PHPS may be converted into SiO_x by two entirely different processes, that is, either by reaction with water, or by a photolytic process in the presence of oxygen. In the presence of water, an oxidative process occurs, which entails the hydrolysis of both the Si–N and Si–H bonds resulting in the release of ammonia and dihydrogen and the formation of silanols (*o*-silicic acid) [Eq. (1)]:[21]

$$-(SiH_2\text{-}NH)_n- + 4n\,H_2O \rightarrow n\,Si(OH)_4 + 2n\,H_2 + n\,NH_3 \quad (1)$$

In a subsequent thermally triggered condensation process, preferably in the presence of a base,[19,20,22] the intermediary formed silanol groups are transformed into an SiO_x network, rendering this approach quite similar to a standard sol–gel process. An alternative route for converting PHPS into SiO_x involves its vacuum ultraviolet (VUV) irradiation[23] in the presence of oxygen. If realized in the absence of water, this approach would allow *the direct formation of Si–O–Si bonds from the progenitor*. Instead of shrinkage, a *volume increase* might be expected, thus allowing the synthesis of a dense coating. Naganuma and co-workers[23] suggested that, rather than the direct impact of high energy photons on chemical bonds, ozone molecules and oxygen radicals $O(^1D)$ generated by the absorption of high-energy photons are responsible for the oxidative transformation of PHPS [Eq. (2)]:

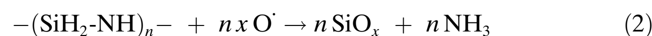

$$-(SiH_2\text{-}NH)_n- \; + \; n\,x\,O^{\cdot} \rightarrow n\,SiO_x \; + \; n\,NH_3 \quad (2)$$

Here, we present a detailed mechanistic study of the conversion of PHPS into SiO_x using different kinds of VUV light, which allow the establishment of a continuous process for the manufacture of SiO_x oxygen and water-vapor-barrier layers. In view of the data retrieved, a different mechanism is presented.

Results and Discussion

Quantum-chemical investigations: Quantum-chemical calculations on the model molecule $NH_2\text{-}SiH_2\text{-}NH\text{-}SiH_3$ revealed that excitation by high-energy VUV photons in fact results in the interconversion to the S_1 singlet state, intersystem crossing to the T_1 triplet state, and subsequent Si–N bond scission (Figure 1). The energy yield for this process is $-19\,kcal\,mol^{-1}$.

The energy gap S_1–S_0 for the absorption threshold was calculated to be 5.63 eV (220 nm). Consequently, photons with wavelengths ≤ 220 nm should be able to trigger Si–N bond scission. Whereas in the ground state the singlet electron of the highest occupied molecular orbital (HOMO) is strongly localized at the nitrogen (n electron), it shifts to the Si atom after excitation and internally crosses to the lowest

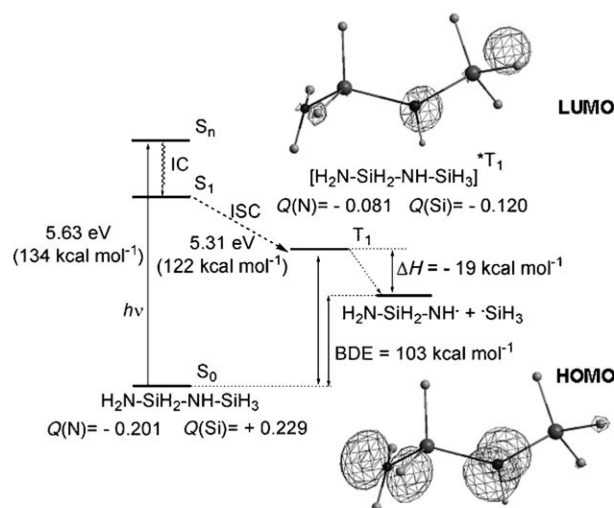

Figure 1. Results of the quantum-chemical calculations on $NH_2\text{-}SiH_2\text{-}NH\text{-}SiH_3$. BDE = bond dissociation energy.

unoccupied orbital (LUMO) (Figure 1). Additionally, the Mulliken atomic charge on the N atom is negative and is positive for Si. This affects a strong Coulomb attraction resulting in a strong Si–N bond. However, transfer of the electron from the HOMO into the LUMO induces a strong intramolecular charge shift. In the course of this process, the Coulomb attraction changes into Coulomb repulsion. This leads to a weakening of the Si–N bond and, in due course, to bond scission. Additional calculations on more complex $-(SiH_2\text{-}NH)_n-$ networks with $n = 6$ again confirmed the VUV excitation of the Si–N bond followed by its scission. Preliminary experiments revealed that VUV irradiation with high-energy photons can in fact accomplish the oxidative decomposition of PHPS layers of some hundred nanometers in thickness within a few minutes, thus superseding the comparably slow hydrolytic cleavage of the Si–N bond by water by at least two orders of magnitude.

Transmission measurements: The results of the VUV transmission measurements on quartz discs spin-coated with PHPS (average thickness of (120 ± 10) nm) by using an uncoated quartz disc as a reference are shown in Figure 2.

Measurements revealed that thermally and VUV-treated PHPS layers are quite similar in terms of their transmission properties. However, their transmission declines to 0.60–0.75 for 164 nm photons. The transmission is even lower for a sample of air-dried parent PHPS. It decreases from about 0.85 at 210 nm to less than 0.10 at 164 nm. From these data it becomes evident that between 210 and 164 nm, photons with *increasing* photon energy are *increasingly* absorbed by PHPS. This is in a good agreement with the above-mentioned calculations on the hypothetical molecule $NH_2\text{-}SiH_2\text{-}NH\text{-}SiH_3$. Thus, during irradiation of a PHPS layer of 120 nm thickness with 172 nm photons, only 10% of the VUV light reaches the bottom of the layer, however, for 185 nm photons this value is already 35%. Calculations of the transmission values of PHPS layers of different thickness

 © 2007 Wiley-VCH Verlag GmbH & Co. KGaA, Weinheim

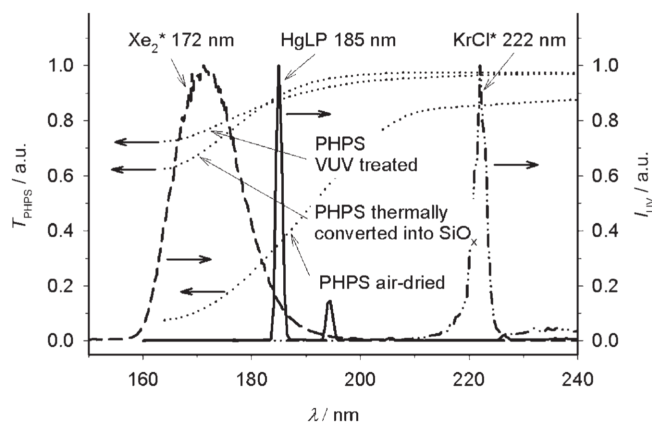

Figure 2. Transmission (T_{PHPS}) of spin-coated PHPS layers (120 nm): air-dried, thermally treated, and VUV-treated (all 120 nm thickness), as well as, emission intensity (I_{UV}) of commercially available VUV lamps versus wavelength (λ): Low-pressure mercury lamp (——); Xe^{2*} excimer lamp (–––); KrCl* excimer lamp (···).

by applying the Beer–Lambert law revealed absorption coefficients of $\varepsilon_{172nm} \approx 8.2\times10^4$ cm^{-1} and $\varepsilon_{185nm} \approx 4.2\times10^4$ cm^{-1}. These values translate into a practically usable penetration depth of VUV photons of about 200 nm for 172 nm photons, and less for shorter wavelengths. However, in the course of the conversion of PHPS into SiO_x, a "bleaching" effect takes place, that is, the molar absorptivity is reduced. This results in an increased penetration depth of the photons with increasing degree of conversion.

In the wavelength range of interest (160–240 nm), three commercially available VUV sources exist: Xenon (Xe_2*) and krypton/chlorine (KrCl*) excimer lamps as well as the mercury low-pressure lamp (HgLP). The emission lines of these lamps with respect to the transmission profiles of pure PHPS and SiO_x are shown in Figure 2. The emission of the Xe_2* excimer lamp covers the range of 160–190 nm, however, with markedly decreasing transmission for decreasing wavelengths, particularly through PHPS, but also through SiO_x. Both the HgLP and the KrCl* excimer lamp have narrowband emissions with full widths at half maximum <3 nm. Besides the 185 nm emission, the main emission peak of the HgLP lamp is located at 254 nm. The emission at 194 nm is of limited importance.

Formation of SiO_x layers from PHPS

VUV sources and degradation kinetics: For evaluation, two-inch Si wafers were spin-coated with PHPS by using 3 wt% solutions in dibutyl ether. The average thickness of the coatings was measured gravimetrically and found to be (120 ± 20) nm. Samples were repeatedly irradiated for 15 s. Xe_2* excimer lamps with various VUV powers of 12 and 30 mW cm^{-2}, HgLP arrays with a VUV power of 12 mW cm^{-2}, and KrCl* excimer lamps with an intensity of 100 mW cm^{-2} were used. Irradiation was carried out within an air-tight irradiation chamber under an N_2 atmosphere enriched with 0.25 vol% of oxygen for trapping the resulting radicals. The gap between the sample surface and the irradiation source was held at 25 mm. After each irradiation step, the IR spectrum was measured in the transmission mode to obtain quantitative information. To eliminate the influence of different layer thicknesses, the IR intensities of all peaks were normalized to the IR intensity of the Si–H peak at 2170 cm^{-1} prior to the first irradiation step. Quantitative evaluation of the Si–H band revealed that upon irradiation with a HgLP module (12 mW cm^{-2}), 92% of the initial amount of PHPS had disappeared within 45 s (see Supporting Information). By using a Xe_2* excimer lamp (12 mW cm^{-2}), 98% of the Si–H bands had disappeared within 30 s. These irradiation times corresponded to VUV energy exposures of 540 and 360 mJ cm^{-2}, respectively. The measured data of the unimolecular decay initiated by VUV photons can be fit by a first-order law with apparent rate constants (k_{app}) for Si–H decomposition of 8.2×10^{-2} s^{-1} and 5.8×10^{-2} s^{-1} for 172 nm and 185 nm irradiation, respectively, applying a light intensity of 12 mW cm^{-2} in either experiment (Figure 3). In contrast, the formation of Si-O-Si bands is much slower (see below for details). These data strongly suggest that Si–N bond scission is *not* related to the reaction

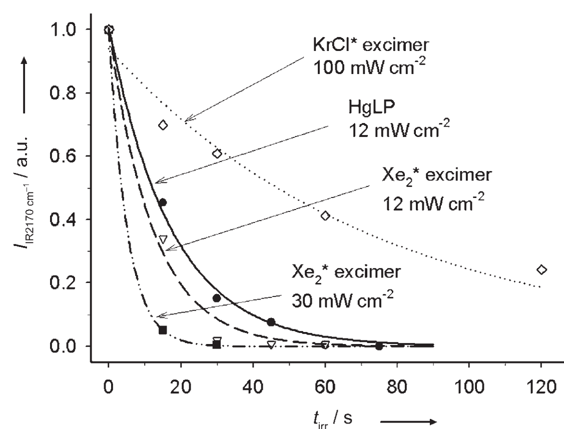

Figure 3. Kinetic data of the intensity of the Si–H vibration band at 2170 cm^{-1} ($I_{IR\,2170\,cm^{-1}}$) after irradiation with VUV light from several sources (t_{irr}: irradiation time).

of PHPS with any form of oxygen (O_2, O_3, O(^{1}D), but triggered photochemically in a preceding reaction (see below). In terms of the mechanism of the VUV degradation of PHPS, these data must be interpreted in that Si–N bonds are broken and, after abstraction of hydrogen from the Si atoms, ammonia is formed. Hence, a decrease in Si–H concentration directly results in a decrease in Si–N concentration. In contrast, the oxidation of the silicon atoms, that is, formation of SiO_x is *not* a simultaneous, but a downstream process. The apparent rate constants for both irradiation experiments run at 12 mW cm^{-2} (Figure 3) also reflect the different degrees of absorption (1–T) of 172 nm (85%) and 185 nm photons (62%) in a 100 nm-thick PHPS layer very well.

 © 2007 Wiley-VCH Verlag GmbH & Co. KGaA, Weinheim

Increasing the VUV power of the Xe_2* lamp from 12 to 30 mW cm^{-2} (factor 2.5), the apparent rate constant for Si–H decomposition rises to $k_{app} = 2.0 \times 10^{-1}$ s^{-1} (factor 2.4) suggesting a linear dependence between the applied dose rate and Si–H decomposition. With the aim to compare irradiation runs at different wavelengths it is expedient to introduce the term "dose actually absorbed by the layer", D_{VUVabs}. Compared to the dose D_{VUVinc} of the incident irradiation, D_{VUVabs} for 172 nm and 185 nm photons by a 100-nm thick PHPS layer is less, that is, 85 and 62 %, respectively, according to the absorption coefficients at these wavelengths. However, the ratio of the apparent rate constant over the dose after 1 min of irradiation, k_{app}/D_{VUVabs}, was $(1.32 \pm 0.02) \times 10^{-4}$ cm^2 s^{-1} mJ^{-1} in all three Xe_2* and HgLP based experiments, suggesting that the entire dose absorbed by the PHPS layer was used for its decomposition. Conversely, irradiation by a KrCl* excimer lamp ($\lambda = 222$ nm) resulted only in an insignificant degradation of the Si–H bond with an apparent rate constant k_{app} of 1.4×10^{-2} s^{-1}. Here, despite an irradiation power of 100 mW cm^{-2}, the power actually absorbed in the thin layer was calculated to be 13 mW cm^{-2}, corresponding to a dose of 780 mJ cm^{-2} after one minute of irradiation. This results in a comparably low ratio k_{app}/D_{VUVabs} of 1.79×10^{-5} cm^2 s^{-1} mJ^{-1}. Thus, these data again nicely confirm both the calculations and transmission measurements and underline the necessity of VUV light <200 nm. In view of these data obtained with the KrCl* excimer lamp, no further experiments were carried out with this source of light.

As described above for Si–H degradation, the process of the Si–O–Si formation was also investigated by FTIR spectroscopy. The (disappearing) peak at 1190 cm^{-1} was assigned to the N–H stretching and bending modes in the Si–NH–Si units, the peak at 1050 cm^{-1} was assigned to the Si–O–Si bonds that were formed.[19] Appropriate experiments for the investigation of the oxidation process were performed by using HgLP (12 mW cm^{-2}) and Xe_2* excimer lamps (12 and 30 mW cm^{-2}, respectively). The kinetic data of the Si–O–Si formation characterized by the IR intensity I at 1050 cm^{-1} can be fit by a first-order law with the resulting equation $I = I_\infty(1 - \exp(-k_{app}t))$, with k_{app}, apparent rate constant [s^{-1}], and I_∞, the extrapolated saturation value (i.e., peak area, [a.u.]) of the Si–O–Si IR peak at $t = \infty$. The latter, again normalized to a layer thickness of 100 nm, was used as the measure for the extent of the oxidative conversion of PHPS to SiO_x. Saturation values for PHPS, thermally converted to SiO_x for 6 h at 215 °C or for 1 h at 600 °C, were 2.11 and 4.77, respectively. Saturation values obtained after irradiation with Xe_2* excimer and HgLP lamps were only 0.75 and 1.25, respectively. From these data it becomes obvious that pure PHPS layers may not be completely converted into SiO_x in the presence of oxygen by VUV irradiation alone.

Influence of oxygen concentration: Next, the influence of the oxygen content in the irradiation atmosphere on the oxidation kinetics was investigated. Because of the steeply rising absorption of VUV photons by O_2 with wavelengths below 185 nm,[24] appropriate experiments were carried out by using a HgLP array (185 nm). As the penetration depth of 185 nm light in oxygen-containing atmospheres is much higher than the penetration depth of 172 nm light, HgLP arrays produce much less ozone than Xe_2* excimer lamps. These facts are elucidated in more detail below in conjunction with the effect of ozone. The volumetric content of oxygen in nitrogen at atmospheric pressure was set to 0.25, 1, 5, and 20 %. The resulting apparent rate constants and saturation values increased with increasing oxygen content, supporting the assumption that reaction kinetics were controlled by oxygen diffusion, which is increasingly hindered by the fast development of a top barrier layer during the course of the conversion process. If this were true, then, at an early stage of conversion, the resulting layers must be expected to consist of basically pure SiO_x at the top and PHPS-derived species that contain N atoms below.

As can be seen in Figure 4, the TOF-SIMS depth profiles do in fact reveal such high conversion of PHPS into SiO_x at the top (0–30 nm) and a lower conversion below, resulting in higher concentrations of Si–N species. However, it has to be clearly stated that these profiles should be discussed in a qualitative and not quantitative way because the changes of roughly one order of magnitude for the detected ion currents are a result of the nonlinear sensitivity of the SIMS. In fact, the TOF-SIMS "overestimates" changes in layer composition, which becomes evident from the saturation values of the Si–O–Si peak (see below). The differences between TOF-SIMS graphs for the irradiations at 172 and 185 nm (the latter not shown) are not pronounced though there is (in accordance with calculations) a slight tendency for a less conspicuous profile in the case of 185 nm irradiation.

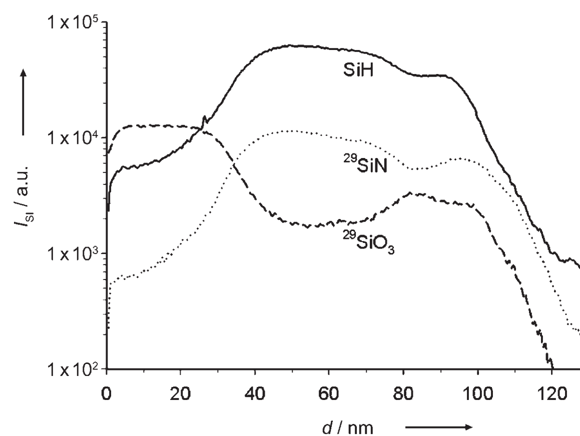

Figure 4. TOF-SIMS depth profiles of spin-coated PHPS layers on Si wafers after VUV treatment with a Xe_2* excimer 2.1 J cm^{-2}. I_{SI}: Intensity of the secondary ion current, d: Penetration depth.

XPS data of the surface of PHPS layers recorded after thermal treatment at 600 °C and after various VUV treatments, revealed that the theoretical Si/O ratio for silica, which is 33:67, was best reached by treatment of PHPS with HgLP lamps applying a dose of 1.30 J cm^{-2}. Thus, a Si/O

 © 2007 Wiley-VCH Verlag GmbH & Co. KGaA, Weinheim

ratio of 33:61 was found for the latter, whilst thermal treatment for 1 h at 600 °C gave only a ratio of 40:59. The balance to 100 was covered by nitrogen from unconverted PHPS and small amounts of carbon resulting from contaminations during sample preparation and/or residual solvent (dibutyl ether).

Base-catalyzed SiO_x formation: As stated above, the formation of SiO_x from PHPS through the VUV-light-triggered process in the presence of oxygen is rather slow. The question of by which means the conversion process from PHPS to silica could be accelerated led to investigations of the impact of organic bases as catalysts. It should be noted that additives like a catalyst may in principle absorb significant portions of the VUV light, thus influencing Si–N decomposition. First, kinetic experiments with tertiary aliphatic amines, for example, dimethylethanolamine (DMEA, $pK_B = 9.9$), diethylethanolamine (DEEA, $pK_B = 10.2$), dimethylpropanolamine ($pK_B = 9.8$), di-2-propylethanolamine ($pK_B = 10.3$), and others (see Experimental Section) were carried out. Nearly all these catalysts caused a spontaneous release of ammonia at concentrations above 1 wt % with respect to the PHPS content in the solution even in the absence of UV light. Only DMEA and DEEA allowed the addition of up to 5 wt % without noticeable release of ammonia. Both DMEA and DEEA gave similar kinetic results with a slight tendency for faster kinetics for DEEA. However, DMEA was the preferred base because of its better classification regarding health and safety regulations. The apparent rate constants for Si–O–Si formation increased from 2.0×10^{-3} to $2.9 \times 10^{-3}\ s^{-1}$ with increasing amounts of catalyst (0–5 wt %, Figure 5, Table 1).

In addition, the saturation value of the Si–O–Si intensity was roughly duplicated reaching the values of thermally converted layers (2.11 for 6 h at 215 °C). Though well known in sol–gel chemistry, this accelerating effect of a base on Si–O–Si formation is somewhat surprising in the present

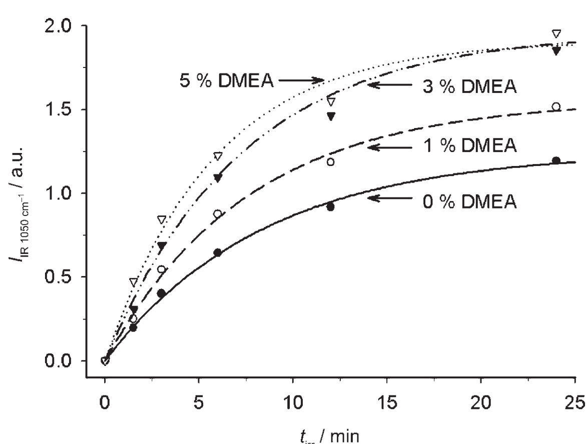

Figure 5. Kinetic data of the UV-irradiation-induced oxidation of PHPS layers with various DMEA content spin-coated onto Si wafers; evaluation on the basis of the intensity of the Si–O–Si vibration peak at $1050\ cm^{-1}$ ($I_{IR\ 1050\ cm^{-1}}$) versus irradiation time (t_{irr}); irradiation by using UV light from a HgLP tube ($12\ mW\,cm^{-2}$), $[O_2] = 0.25$ vol %.

Table 1. Apparent rate constant k_{app} of the Si–O–Si appearance and saturation value (SV) of the Si–O–Si band at $1050\ cm^{-1}$ for irradiation of PHPS with UV light from a HgLP tube ($12\ mW\,cm^{-2}$), $[O_2] = 0.25$ vol %, at different DMEA concentrations.

[DMEA]/[wt %]	Rate constant $k_{app}/[s^{-1}]$	Saturation value SV/[a.u.]
0	1.97×10^{-3}	1.25
1	2.19×10^{-3}	1.56
3	2.29×10^{-3}	1.97
5	2.89×10^{-3}	1.91

system, because experiments were carried out in the absence of water ($[H_2O] < 25$ ppm). So far, we have been unable to come up with a rational mechanistic explanation for these findings. However, one might argue that tertiary amines might be involved in oxygen-transfer processes. In this context, it is important to note that the decomposition of PHPS was found to be zero order in base, that is, addition of a catalyst did *not* influence the decomposition of the Si–N bond, which solely depended on the irradiation dose. Vice versa, Si–O–Si formation at the beginning of the oxidation process was found to be roughly first order in base and first order in oxygen. At concentrations > 5 wt %, DMEA noticeably absorbs the VUV photons leading to an *apparent* decrease of the rate constant of the Si–H decay by reducing the applied dose.

Depth profiles: Owing to the wavelength dependence of the penetration depth of UV light (Figure 2), the question of depth profiles for oxygen and nitrogen came to the fore. Samples of PHPS spin-coated on Si wafers (100 nm coating) and exposed to VUV light for different irradiation times were investigated by using time-of-flight secondary ion mass spectrometry (TOF-SIMS), which allowed the determination of such profiles by alternating coplanar depth sputtering and measurement of the secondary ions (Figure 6).

It is evident that the profiles for both the $^{29}SiN^-$ and the $^{29}SiO_3^-$ ions are different for different irradiation times. A thin surface layer (< 20 nm) consisting of partially hydrolyzed PHPS forms during sample preparation and transport. Here, at $t = 0$ min, the concentration of $^{29}SiN^-$ in parent PHPS is still high, whereas the concentration of $^{29}SiO_3^-$ is comparably low. After 3 min, the top layer shows a decreased concentration of $^{29}SiN^-$ and an increased concentration of $^{29}SiO_3^-$, a process, which becomes more pronounced after ten minutes. Finally, after 24 minutes, both profiles are virtually homogeneous showing low N atom and high O atom concentrations, thus illustrating the complete conversion of PHPS into SiO_x. The discontinuities on the right side of either chart are caused by the underlying Si wafer surface.

Role of ozone: Finally, we tried to shed some light on the role of ozone that may be formed as a by-product at comparably high concentrations during the course of the irradiation process. This appears to be prudent, especially as ozone has been suggested to be one of the active species responsi-

 © 2007 Wiley-VCH Verlag GmbH & Co. KGaA, Weinheim

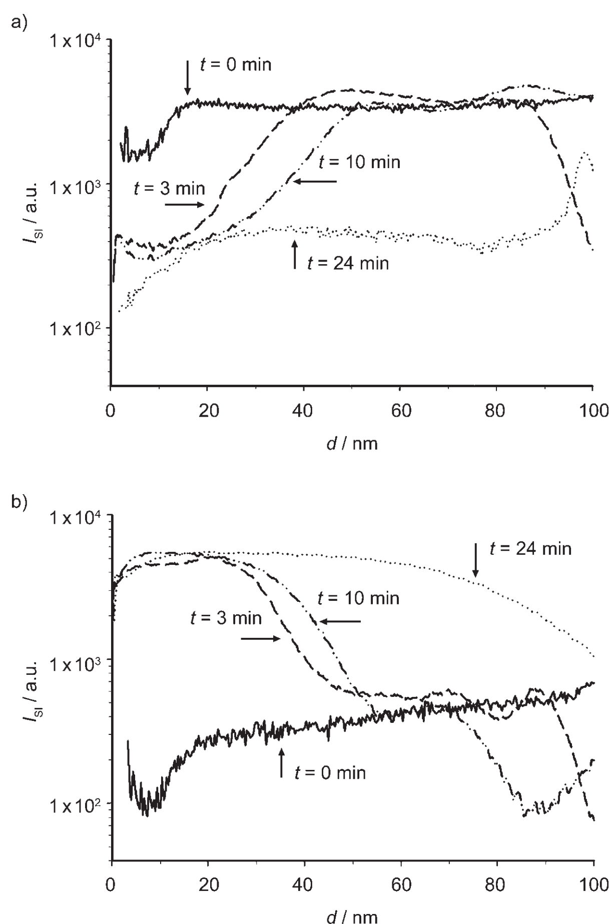

Figure 6. TOF-SIMS depth profiles of spin-coated PHPS layers on Si wafers UV treated with a HgLP array for 0, 3, 10, and 24 min, respectively. I_{SI}: Intensity of the secondary ion current, d: Penetration depth. a) Profiles for $^{29}SiN^-$; b) profiles for $^{29}SiO_3^-$ (curves normalized to the $^{29}SiN^-$ value at 72 nm.

ble for PHPS conversion.[23] First, experiments with ozone produced by an external ozone generator and added to the atmosphere were carried out. Samples were exposed to 500 or 2600 ppm of ozone in the absence of any VUV irradiation for five minutes. Subsequent analysis by IR spectroscopy revealed only a negligible oxidation of the PHPS layers, that is, only a small increase of the Si–O–Si band at 1050 cm^{-1} was observed. The addition of ozone under simultaneous irradiation with HgLP lamps with narrowband VUV emission at (185 ± 3) nm did *not* cause a conspicuous accelerating effect on the oxidation process of PHPS compared to those experiments carried out in the presence of oxygen yet in the absence of additional (externally generated) ozone. To rationalize these findings, one needs to know that: 1) 254 nm light present in HgLP lamps decomposes ozone into O_2 and $O(^1D)$ radicals and; 2) 172 nm light generated by Xe_2* lamps generates ozone from oxygen through intermediate formation of $O(^1D)$, a process that occurs to a very minor extent with 185 nm light. In other words, addition of ozone under *simultaneous irradiation* with HgLP lamps leads to a simultaneous exposure of the sample to both VUV irradiation and $O(^1D)$/ozone impact, whereas treatment with HgLP lamps in the presence of oxygen alone does not generate significant amounts of $O(^1D)$ or ozone. This means that neither ozone nor $O(^1D)$ can be responsible for the degradation of PHPS. Conversely, addition of 500 or 2600 ppm ozone and the use of radiation >250 nm would generate a situation in which the sample was only exposed to $O(^1D)$ and ozone, but not to any radiation <200 nm. Such wavelengths around 250 nm were easily realized by using a standard HgLP lamp made from a quartz that suppresses VUV light. In fact, the oxidation proceeded very slowly and to a very minor extent, if at all. From these findings and the fact that Si–H (Si–N) decomposition is much faster than Si–O–Si formation (see above), we conclude that, under the conditions used for the experiments presented here, the reaction of PHPS with oxygen proceeds rather through scission of the Si–N bond by VUV light followed by reaction of Si radical species with oxygen than through direct reaction of PHPS with $O(^1D)$ or ozone. This is in contrast to the findings for the Xe_2* irradiation of PHPS reported by Naganuma and co-workers[23] and needs clarification. Because the absorption coefficient of O_2 for 185 nm photons is about two orders of magnitude smaller than that for 172 nm photons (0.2 instead 15 cm^{-1}[24]), hardly any ozone is formed from O_2 in the presence of 185 nm light. In addition, the 172 nm emission of the Xe_2* excimer lamp is characterized by a comparably wide wavelength range from 160 to 190 nm for which a change of the absorption coefficient from 130 to 0.08 cm^{-1} results (more than three orders of magnitude). Consequently, different penetration depths in oxygen are found for different parts of the spectrum. These range from 0.4 mm to 60 cm in dry air for 160 nm and 190 nm photons, respectively. Even a 20 mm gap of dry air as used in the experiments reported by Naganuma and co-workers[19] only absorbs 85 % of the entire VUV irradiation from a Xe_2* excimer lamp. This value is based on a calculation by using the oxygen absorption coefficients published by Watanabe and co-workers,[24] as well as, the intensities of the Xe_2* excimer emission spectrum shown in Figure 2. In the experiments of Naganuma,[19] the impact of VUV radiation was not excluded and the formation of Si–O–Si bonds was not necessarily caused by $O(^1D)$/ozone impact alone as intended. In view of these data and our findings we suggest a modified reaction scheme that illustrates that irradiation of VUV light is mainly responsible for the cleavage of the Si–N bond and, the Si–H bonds in PHPS [Eq. (3)]:

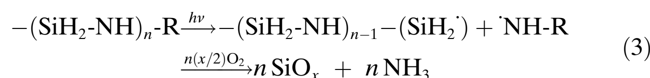

$$-(SiH_2\text{-}NH)_n\text{-}R \xrightarrow{h\nu} -(SiH_2\text{-}NH)_{n-1}-(SiH_2^{\cdot}) + {}^{\cdot}NH\text{-}R \xrightarrow{n(x/2)O_2} n\,SiO_x + n\,NH_3 \quad (3)$$

The radical Si species that form during the course of this reaction are proposed to react with oxygen and finally form the final SiO_x network. Detailed electron spin resonance (ESR) studies that will shed light on intermediary formed reactive species, for example, Si–O and Si–OH radicals are under way.

 © 2007 Wiley-VCH Verlag GmbH & Co. KGaA, Weinheim

Oxygen barriers: To determine the oxygen barrier properties, solutions of PHPS in dibutyl ether (1.5 and 3.0 wt %, respectively) enriched with 5 wt % of DMEA with respect to PHPS were used for the coating of 23 μm PET foils. Corona treatment was used prior to the coating process to ensure sufficient adhesion between the PET foil and the SiO_x layer to be created. The coating process was carried out from roll to roll by slit-nozzle-coating using a coating machine with a band speed of 7.5 $m\,min^{-1}$. The average layer thickness was adjusted by volumetric dosage by using a gear pump within a range of 200–500 nm ±10 % and confirmed gravimetrically. VUV light generated by HgLP tubes and/or Xe_2* excimer lamps was applied under an N_2 atmosphere enriched with 0.25–5 vol % of oxygen. Oxygen transmission rates (OTRs) and barrier improvement factors (BIFs) obtained with such PHPS-derived coatings are summarized in Table 2.

Table 2. Summary of OTR and BIF values for differently converted PHPS-coated PET samples. The OTR value of the parent PET foil was 80 $cm^3\,m^{-2}\,d^{-1}\,bar^{-1}$.

Process[a]	VUV source	Dose [$mJ\,cm^{-2}$]	d[b]	OTR[c]/BIF	[O_2] [vol %]
stationary	Xe_2*	2.1	300	0.20/400	0.25
stationary (double layer)	Xe_2*	2.1	300	<0.10/>800	0.25
continuous	HgLP + Xe_2*	0.66	310	1.7/47	5/0.25
continuous	HgLP + Xe_2*	0.33	310	4.0/20	5/0.25

[a] 1.5 wt % PHPS in dibutyl ether, 5 wt % DMEA. [b] Layer thickness in nm. [c] In $cm^3\,m^{-2}\,day^{-1}\,bar^{-1}$.

As can be seen, OTR values of 1.7 $cm^3\,m^{-2}\,day^{-1}\,bar^{-1}$, corresponding to a BIF of 47 were achieved in a continuous process by one single coating. In stationary experiments, OTR values down to 0.20 $cm^3\,m^{-2}\,day^{-1}\,bar^{-1}$, corresponding to a BIF up to 400, were achieved. Creating a double layer with a total thickness of 300 nm decreased the OTR value to 0.10 $cm^3\,m^{-2}\,day^{-1}\,bar^{-1}$, corresponding to a BIF of up to 800. It is worth mentioning that the coated foils remained fully flexible and transparent.

Conclusion

In summary, the water-free VUV-triggered process of converting PHPS into SiO_x in the presence of O_2 has been elucidated. The investigations presented here therefore open up the possibility for both the batchwise and continuous production of barrier layers on polymeric substrates at ambient temperature and pressure and may well be expected to positively influence the technology of flexible OLEDs and organic solar cells.

Further investigations will focus on the clarification of the oxidation mechanism after the photolysis of the Si–N bonds.

Experimental Section

PHPS was obtained from Clariant GmbH as a 20 wt % solution in dibutyl ether (DBE). It is of utmost importance to check the quality of the PHPS solution because significant hydrolysis may occur during storage in the presence of moisture. ***CAUTION: Solutions stored for long periods of time may develop explosive mixtures of silanes!*** All measurements were carried out on spin-coated 2- or 3-inch silicon wafers. For spin-coating, a 3 wt % solution of PHPS was prepared by further dilution with DBE and addition of the appropriate amount of catalyst. The following catalysts were tested: 2-(dimethylamino)ethanol (DMEA), 2-(diethylamino)ethanol (DEEA), 1-(dimethylamino)-2-propanol (DMiPA), 1,8-diazabicyclo[5.4.0]undec-7-ene (DBU), all from Merck (Darmstadt, Germany), 3-(dimethylamino)-1-propanol (DMPA), 2-(di-2-propylamino)-ethanol (DiPEA), 1,5,7-triazabicyclo[4.4.0]dec-5-ene (TBD), 1,4-diazabicyclo[2.2.2]octane (DABCO), phosphazene P_4-t-Oct, all from Fluka (Taufkirchen, Germany). Spin-coating was carried out at different speeds (300–3000 rpm) for 1 min. To cover a thickness range of 50–300 nm, up to three subsequent coatings were carried out. After coating, samples were dried at room temperature under air for at least 30 min to obtain a solvent-free PHPS layer. PHPS was transformed into SiO_x either by thermal treatment or by irradiation with UV or VUV light. Two types of Xe_2* excimer lamps were used as VUV sources: a 172/630 Z lamp system (Heraeus Noblelight GmbH, Kleinostheim, Germany), applying a VUV power of up to 30 $mW\,cm^{-2}$ and a XERADEX 20 L40/120 system (Radium Lampenwerk GmbH, Wipperfürth, Germany) with a VUV power of 12 $mW\,cm^{-2}$. Additionally, an irradiation module consisting of two low-pressure mercury lamps (HgLP) UVI80 U S 15/395 (uv-technik Speziallampen GmbH, Wümbach, Germany, 12 $mW\,cm^{-2}$) was adopted. Irradiation was carried out in an irradiation chamber flushed with dinitrogen (Air Products, Hattingen, Germany), containing defined concentrations of oxygen in the range of 25 vppm to 20.6 vol %. The gap between radiation source and sample surface was 26 mm in all cases. Additional UV sources were a KrCl* excimer tube 222/635 Z (Heraeus Noblelight GmbH, narrowband emission at 222 nm) and a medium-pressure mercury lamp (HgMP, IST GmbH, Nürtingen, Germany). VUV/UV emission spectra were measured by using a VUV/UV spectrometer VM 502 (Acton Research Corp., Acton, USA). FTIR spectra were recorded on an IFS 55 instrument (Bruker GmbH, Karlsruhe, Germany) in the transmission mode. Transmission measurements of quartz discs (Suprasil 2, diameter 1 inch, thickness 2 mm, Aachener Quarz-Glas Technologie Heinrich, Aachen, Germany) spin-coated with PHPS in the VUV/UV range were accomplished at the Physikalisch-Technische Bundesanstalt Berlin, Germany, on a beam line of the BESSY synchrotron. OTRs were measured on OX-TRAN Models 2/21 (MOCON, Minneapolis, Minnesota, USA) at 0 % relative humidity and 23 °C.

TOF-SIMS measurements: TOF-SIMS spectra were recorded on a TOF-SIMS V system (ION-TOF GmbH, Münster, Germany). Depth profiles of the layers were produced by applying a Cs ion beam (0.5 keV, 40 nA). Ablation was carried out in a planar way for 3 s on an area of 300 × 300 μm^2 by applying an ablation rate of approximately 6 $nm\,min^{-1}$. Within this pre-etched region, an area of 50 × 50 μm^2 was excited by a Ga ion beam (15 keV, 25 nA), which produced secondary ions that were analyzed by using a coupled mass spectrometer (negative-ion mode). By iteration of sputter-etching and concentration analysis, intensity profiles of different secondary ion species versus etching time were produced. After measurements, the etched craters were sized by using a white light interference microscope MICROMAP 128/512 (ATOS GmbH, Pfungstadt, Germany). In this way the depth was related to the etching time.

Quantum-chemical calculations: Quantum-chemical calculations were carried out by using the Gaussian 03 package. For the systems under study, geometries were optimized by applying the density functional theory (DFT) approach with B3LYP hybrid functionals.[25–27] Molecular orbitals (MOs) were visualized in graphical form with the help of the GaussView 2.1 program.[28,29] For geometry optimizations, the standard 6-31G(d,p) basis sets were used. The electronic transition spectra of transients were calculated with the unrestricted time-dependent (UTD

© 2007 Wiley-VCH Verlag GmbH & Co. KGaA, Weinheim

DFT)[29] B3LYP/6-31+G(d,p) method. X-ray diffraction measurements were carried out by using an XRD 3003 PTS instrument (Seifert, Ahrensburg, Germany).

Determination of PHPS concentration: Hydrochloric acid (0.25 m, 50 mL) and 1,4-dioxane (10 mL, as solubilizer) were placed in a 200 mL Erlenmeyer flask with a ground joint. To this mixture, PHPS solution (1.000 mL = 0.8270 g, about 20 wt% in dibutyl ether) was added. Immediately after PHPS addition, the Erlenmeyer flask was sealed to be gas-tight with a ground glass stopper covered with a Teflon sealing and locked with a clamp. Then, the resulting mixture was intensively stirred for 1 h. A few drops of bromothymol-blue (0.1 wt% in 20 vol% aqueous ethanol) were added to the solution. The excess of hydrochloric acid was back-titrated by using a 0.25 M sodium hydroxide solution (color change from yellow to blue).

Acknowledgements

This work was supported by the Bundesministerium für Bildung und Forschung, BMBF (contract no. 01RI06007). The authors are grateful to Prof. Dr. M. Richter, Physikalisch-Technische Bundesanstalt, Berlin, for VUV transmission measurements on the beam-line of the BESSY synchrotron.

[1] M. Z. Asuncion, R. M. Laine, *Macromolecules* **2007**, *40*, 555.
[2] Z. Harmati, D. Hegemann, *Materialwiss. Werkstofftech.* **2005**, *36*, 198.
[3] A. Shirakura, M. Nakaya, Y. Koga, H. Kodama, T. Hasebe, T. Suzuki, *Thin Solid Films* **2005**, *494*, 84.
[4] N. S. Sangaj, V. C. Malshe, *Prog. Org. Coat.* **2004**, *50*, 28.
[5] H. Chatham, *Surf. Coat. Technol.* **1996**, *78*, 1.
[6] K. Teshima, Y. Inoue, H. Sugimura, O. Takai, *Vacuum* **2002**, *66*, 353.
[7] Y. Leterrier, *Progr. Mater. Sci.* **2003**, *48*, 1.
[8] J. Madocks, J. Rewhinkle, L. Barton, *Mater. Sci. Eng. B* **2005**, *119*, 268.
[9] F. Kessler, D. Herrmann, M. Powalla, *Thin Solid Films* **2005**, *480*, 491.
[10] D. Pech, P. Steyer, A. S. Loir, J. C. Sanchez-Lopez, J. P. Millet, *Surf. Coat. Technol.* **2006**, *201*, 347.
[11] T. N. Chen, D. S. Wuu, C. C. Wu, C. C. Chiang, Y. P. Chen, R. H. Horng, *J. Electrochem. Soc.* **2006**, *153*, F244.
[12] D. S. Wuu, W. C. Lo, C. C. Chiang, H. B. Lin, L. S. Chang, R. H. Horng, C. L. Huang, Y. J. Gao, *Surf. Coat. Technol.* **2005**, *197*, 253.
[13] J. Fricke, H. Schwab, U. Heinemann, *Int. J. Thermophys.* **2006**, *27*, 1123.
[14] K. Reichelt, X. Jiang, *Thin Solid Films* **1990**, *191*, 91.
[15] A. Bieder, A. Gruniger, P. R. v. Rohr, *Surf. Coat. Technol.* **2005**, *200*, 928.
[16] A. G. Erlat, B. C. Wang, R. J. Spontak, Y. Tropsha, K. D. Mar, D. B. Montgomery, E. A. Vogler, *J. Mater. Res.* **2000**, *15*, 704.
[17] S. Iwamori, Y. Gotoh, K. Moorthi, *Surf. Coat. Technol.* **2003**, *166*, 24.
[18] T. P. Chou, C. Chandrasekaran, G. Z. Cao, *J. Sol-Gel Sci. Technol.* **2003**, *26*, 321.
[19] K. Kamiya, T. Tange, T. Hashimoto, H. Nasu, Y. Shimizu, *Res. Rep. Fac. Eng. Mie Univ.* **2001**, *26*, 23.
[20] F. Bauer, U. Decker, A. Dierdorf, H. Ernst, R. Heller, H. Liebe, R. Mehnert, *Prog. Org. Coat.* **2005**, *53*, 183.
[21] H. Kriegsmann, G. Engelhardt, *Z. Anorg. Allgem. Chem.* **1960**, *310*, 100.
[22] T. Kubo, E. Tadaoka, H. Kozuka, *J. Mater. Res.* **2004**, *19*, 635.
[23] Y. Naganuma, S. Tanaka, C. Kato, T. Shindo, *J. Ceram. Soc. Jpn.* **2004**, *112*, 599.
[24] K. Watanabe, C. Edward, C. Y. Inn, M. Zelikoff, *J. Chem. Phys.* **1953**, *21*, 1026.
[25] A. D. Becke, *J. Chem. Phys.* **1993**, *98*, 5648.
[26] A. D. Becke, *J. Chem. Phys.* **1996**, *104*, 1040.
[27] C. Lee, W. Yang, R. G. Parr, *Phys. Rev. B* **1987**, *37*, 785–789.
[28] Gaussian 03 (Revision A.1), M. J. Frisch, G. W. Trucks, H. B. Schlegel, G. E. Scuseria, M. A. Robb, J. R. Cheeseman, J. A. Montgomery, Jr., T. Vreven, K. N. Kudin, J. C. Burant, J. M. Millam, S. S. Iyengar, J. Tomasi, V. Barone, B. Mennucci, M. Cossi, G. Scalmani, N. Rega, G. A. Petersson, H. Nakatsuji, M. Hada, M. Ehara, K. Toyota, R. Fukuda, J. Hasegawa, M. Ishida, T. Nakajima, Y. Honda, O. Kitao, H. Nakai, M. Klene, X. Li, J. E. Knox, H. P. Hratchian, J. B. Cross, C. Adamo, J. Jaramillo, R. Gomperts, R. E. Stratmann, O. Yazyev, A. J. Austin, R. Cammi, C. Pomelli, J. W. Ochterski, P. Y. Ayala, K. Morokuma, G. A. Voth, P. Salvador, J. J. Dannenberg, V. G. Zakrzewski, S. Dapprich, A. D. Daniels, M. C. Strain, O. Farkas, D. K. Malick, A. D. Rabuck, K. Raghavachari, J. B. Foresman, J. V. Ortiz, Q. Cui, A. G. Baboul, S. Clifford, J. Cioslowski, B. B. Stefanov, G. Liu, A. Liashenko, P. Piskorz, I. Komaromi, R. L. Martin, D. J. Fox, T. Keith, M. A. Al-Laham, C. Y. Peng, A. Nanayakkara, M. Challacombe, P. M. W. Gill, B. Johnson, W. Chen, M. W. Wong, C. Gonzalez, J. A. Pople, Gaussian, Inc., Pittsburgh, PA, **2003**..
[29] R. Bauernschmitt, R. Ahlrichs, *Chem. Phys. Lett.* **1996**, *256*, 454.

Received: March 2, 2007
Published online: July 18, 2007

 © 2007 Wiley-VCH Verlag GmbH & Co. KGaA, Weinheim